An Alternative Model of Tubulobulbar Complex Internalization During Junction Remodeling in the Seminiferous Epithelium of the Rat Testis 1

Authors: Lyon, Kevin R.P., Bosseboeuf, Emy, and Vogl, A. Wayne

Source: Biology of Reproduction, 93(1)

Published By: Society for the Study of Reproduction

URL: https://doi.org/10.1095/biolreprod.115.128942

BIOLOGY OF REPRODUCTION (2015) **93**(1):12, 1–11
Published online before print 3 June 2015.
DOI 10.1095/biolreprod.115.128942

An Alternative Model of Tubulobulbar Complex Internalization During Junction Remodeling in the Seminiferous Epithelium of the Rat Testis[1]

Kevin R.P. Lyon,[3] Emy Bosseboeuf,[3,4] and A. Wayne Vogl[2,3]

[3]*Department of Cellular and Physiological Sciences, Faculty of Medicine, University of British Columbia, Vancouver, Canada*
[4]*Unité de Formation Biologie Santé, Université de Poitiers, France*

ABSTRACT

Tubulobulbar complexes (TBCs) are elongate subcellular machines responsible for internalizing intercellular junctions during sperm release. Each complex consists of a double-membrane tubular core terminating in a clathrin-coated pit. The core is surrounded by a network of actin filaments, and a distinct swelling or bulb, which lacks an association with actin, develops in the distal third of the structure. The bulb eventually buds from the complex and enters endocytic compartments of the Sertoli cell. The relationship of the actin cuff to the formation and budding of the bulb is not known. To gain insight into this relationship, we perturbed the actin networks of TBCs with cytochalasin D. When isolated testes were perfused with a physiological buffer containing cytochalasin D, apical TBCs at stage VII of spermatogenesis were associated with lower levels of actin compared to controls. At the ultrastructural level, the actin networks in cytochalasin D-treated testes appeared patchy, and ectopic bulbs and swollen tubular regions occurred. When normal untreated samples at early stage VII were analyzed, large elongate bulbs and short tubular sections were observed. Together, these results suggest a new model for TBC vesiculation in which the actin network begins to disassemble and the tubular region begins to swell into a bulb. As actin disassembly continues, the coated pit and most of the tubular region are incorporated into the enlarging bulb. The remaining short neck of the bulb near the base of the complex undergoes scission, and the bulb is internalized.

actin networks, junction remodeling, seminiferous epithelium, Sertoli cells, spermatogenesis, testis, tubulobulbar complex

INTRODUCTION

Intercellular junction remodeling during spermatogenesis is critical to the normal production of spermatozoa by the mammalian testis. In basal regions of the seminiferous epithelium, massive junction complexes between neighboring Sertoli cells disassemble above and reassemble below the next generation of spermatogenic cells as they move from basal to adluminal compartments of the epithelium [1]. Tight junctions within these complexes contribute to the blood-testis barrier [2]. In apical regions, junctions between Sertoli cells and mature spermatids disassemble to release the latter cells, as spermatozoa, into the duct system, while at the same time new junctions form between Sertoli cells and early elongating spermatids deeper in the epithelium. Fundamental to the process of junction remodeling in the seminiferous epithelium are structures termed tubulobulbar complexes (TBCs).

TBCs are proposed to be subcellular machines that internalize intercellular junctions during junction turnover [3–5]. They form only at intercellular junctions in the testis, and their appearance precedes sperm release [6] and spermatocyte translocation [7]. Multiple generations of complexes form as junctions disassemble [8], and the structures often occur in clusters, particularly at apical sites of attachment between Sertoli cells and spermatids [9]. In rats, as many as two dozen complexes occur in Sertoli cell regions adjacent to the convex face of each mature hook-shaped spermatid head at stage VII of spermatogenesis prior to sperm release at stage VIII [6].

Each TBC consists of an elongate tubular extension of either a Sertoli cell or a spermatid that projects into a corresponding invagination of the adjacent Sertoli cell [6]. The double-membrane core of the complex is cuffed by an actin (ACT-) filament network and the distal end of the structure is capped by a clathrin (CLT-)-coated pit [10]. A swollen region or ''bulb'' forms near the end of the complex. The bulb, which lacks an actin cuff and is closely related to cisternae of endoplasmic reticulum, eventually loses its association with the complex and enters endocytic compartments of the Sertoli cell [6].

TBCs have some structural and molecular similarities to podosomes that occur in other cells [11] and to membrane tubules that develop in cell-free systems [12]. They also have a protein domain profile that mirrors that of clathrin-mediated endocytosis machinery present in cells generally [3, 4, 13–15]. In fact, except for their double-membrane cores and the presence of bulbs, TBCs resemble clathrin-coated pits with very long necks.

The function of the actin filament cuffs at TBCs is not entirely clear, although a role in the formation and maintenance of tubular regions appears likely. Knocking down cortactin (CTTN), a key regulator of actin filament/membrane dynamics in other systems [16, 17], results in shorter TBCs than in controls [18]. When the actin filament disruptor cytochalasin D is injected into the testis, typical TBCs do not occur; rather, elongate tubular regions and bulbs are completely absent and only the double-membrane coated pits occur directly at sites of Sertoli cell attachment to spermatids [19]. Both of these results are consistent with the actin networks playing a role in the

[1]Supported by a grant (#155397-2013) to A.W.V. from the Natural Sciences and Engineering Research Council (NSERC) of Canada Discovery Grant Program. Presented in part at the ASCB conference, December 2014, Philadelphia, Pennsylvania, and at the FASEB conference, March 2015, Boston, Massachusetts.
[2]Correspondence: A. Wayne Vogl, Department of Cellular and Physiological Sciences, Life Science Centre, 2350 Health Sciences Mall, University of British Columbia, Vancouver, BC, Canada V6T 1Z3. E-mail: vogl@mail.ubc.ca

Received: 6 February 2015.
First decision: 2 March 2015.
Accepted: 26 May 2015.

eISSN: 1529-7268 http://www.biolreprod.org
ISSN: 0006-3363

formation of TBCs. Details about how the bulbs form in relationship to the actin cuffs and how the bulbs ''bud'' from TBCs are not known. Also not known are the fates of the coated pits and the remaining tubular elements of the complexes, although, like the bulbs, they have been assumed to undergo some form of scission or vesiculation and to be internalized by the Sertoli cell [6, 20].

Here we revisit perturbing actin filament networks in the testis with cytochalasin D, but use the ex vivo testis perfusion technique pioneered by Hoffer and coworkers [21], rather than intratesticular injection as introduced by Russell and coworkers [22], to better control dosages. Over the period of an hour, cytochalasin D significantly altered but did not eliminate the actin filament networks of TBCs at stage VII of spermatogenesis. Using fluorescence thresholding techniques as an index of the amount of actin network present in regions containing the complexes, less actin was present after cytochalasin treatment than in controls. At the ultrastructural level, the actin networks appeared patchy and concentrated into foci. Tubular regions were swollen, ectopic bulb regions were present, and the complexes were shorter and often malformed. Based on these results and on the observations of normal untreated TBCs in early stage VII of spermatogenesis, we propose a new model for the formation and budding of bulbs that involves progressive loss of the actin filament networks that enables the initiation and growth of the bulbs, and the presence of a single scission site at the base of each complex.

MATERIALS AND METHODS

Animals

Reproductively active male Sprague Dawley rats (*Rattus norvegicus)* obtained from Charles River were used in all experiments. Animals were housed and used in accordance with guidelines established by the Canadian Council on Animal Care and according to protocols approved by the Animal Care Committee of the University of British Columbia, and according to the Society for the Study of Reproduction specific guidelines and standards. A total of seven animals were used for this study with two (one for fluorescence and one for electron microscopy) used for each of the 10 and 20 μM experiments and three (two for fluorescence and one for electron microscopy) for the 40 μM experiments.

Reagents

Unless otherwise indicated, all reagents used were obtained from Sigma-Aldrich.

Organ Perfusion

The ex vivo perfusion protocol used in this study was similar to that published by Hoffer and coworkers [21]. Testes were excised from rats that were under deep anesthesia induced by isoflurane inhalation. For each experiment, one testis was used for cytochalasin D treatment, and the other testis from the same animal when possible was used as a control. The spermatic artery of each testis was cannulated with a 27-gauge syringe needle attached to the outlet port of a three-way valve. One of the delivery ports was attached by tubing to a two-channel peristaltic pump calibrated to deliver 1 ml/min of treatment or control solution. The other port of the valve was attached by tubing to a bottle suspended above the table and set to deliver fixative by gravity feed. Flasks containing treatment and control buffers were housed in a water bath set to 33°C and were aerated with 5% CO_2 in O_2. Fixatives also were warmed to 33°C prior to being used. Treatment and control solutions were made up in Krebs-Henseleit buffer containing 4% bovine serum albumin. Treatment solutions contained cytochalasin D (at 10, 20, or 40 μM) added from a stock concentration of 20 or 40 mM in dimethyl sulfoxide (DMSO). Control solutions contained the same volume of DMSO as added to the treatment solutions.

Testes were perfused for 1 h with treatment or control solutions followed by perfusion with fixative for 30 min.

We initially explored using latrunculin A to perturb actin at TBCs, but did not observe any obvious effects when the organ was perfused for 1 h at a concentration of 0.2 μM. We did not pursue this approach further and proceeded to use cytochalasin D, which had an observable effect.

Fluorescence Microscopy

For analysis by fluorescence microscopy, testes were perfused with a fixative containing 3% paraformaldehyde, 150 mM NaCl, 4 mM Na/PO_4, and 5.0 mM KCl, and adjusted to pH 7.3. Treatment and control testes were removed from the needles and cut in half. One half of each testis was used for preparing cryosections and the other half was used for preparing epithelial fragments.

For preparing cryosections, the sample was placed in a small pool of Optimal Cutting Temperature Compound (Sakura Finetek USA) on the top of an aluminum stub and frozen using liquid nitrogen. Sections (5 μm thick) were cut on a cryomicrotome and collected onto slides coated with poly-L-lysine. The slides were immediately submerged in cold acetone (−20°C) for 5 min and air dried.

For preparing epithelial fragments, half of each testis was placed into a Petri dish containing PBS (150 mM NaCl, 4 mM Na/K PO_4, 5 mM KCl, pH 7.3), the capsule was removed, and the seminiferous tubule mass was cut into small pieces using scalpels. The pieces in the PBS were transferred into 50-ml tubes and gently aspirated once through an 18-gauge needle followed by a 21-gauge needle attached to a 10-ml syringe. The fragments were transferred into a 15-ml tube and allowed to settle for 5 min. During this time, larger tubule fragments settled to the bottom of the tube and smaller epithelial fragments containing mature spermatids with associated Sertoli cell apical processes remained suspended in solution. The suspended material was transferred to another 15-ml tube and centrifuged at low speed on a tabletop centrifuge to pellet the epithelial fragments. The supernatant was removed and the pellet gently resuspended in a small volume of PBS. These fragments were then transferred to poly-L-lysine-coated slides. The fragments were allowed to settle and attach to the slide for 10 min inside a humidity chamber. Excess fluid was removed and the slides were immediately submerged in cold acetone (−20°C) for 5 min and then air dried.

Epithelial fragments and cryosections were rehydrated with PBS containing 0.05% Tween 20 (TPBS) and 0.1% BSA for 20 min at room temperature. The tissue was stained with phalloidin conjugated to Alexa Fluor 488 (Invitrogen) for 30 min in a humidity chamber followed by two washes with TPBS/0.1% BSA for 10 min each. The slides were mounted using Vectashield containing 4′,6-diamidino-2-phenylindole (DAPI; Vector Laboratories).

Sections and fragments were imaged using a conventional fluorescence microscope (Zeiss Axiophot) with a film camera. Conditions in which the experimental and control sections and fragments were photographed were kept the same to allow for comparison of the signal intensity. All of the film for one experiment and its controls were developed in the same developer and fixative together. The images were then digitally scanned at 6400 dpi for quantification. The raw image obtained was used for quantification and the images used for illustration purposes were adjusted identically in Adobe Photoshop CS6.13 using the levels function without altering the integrity of the data.

Fluorescence Quantification of Actin Staining at TBCs

Only images of intact apical processes containing stage VII spermatids with associated apical processes of Sertoli cells from fragmented tissue were used in the quantification analysis. The process used to get an index of the area occupied by the actin networks at TBC clusters was carried out using ImageJ software version 1.48 [23]. All spermatids used for quantification were rotated to have the same orientation. For each experiment, controls were used to set the appropriate threshold value that would best represent only the staining of the actin networks at TBC clusters. This threshold was then applied to all spermatids analyzed in that specific experiment. The analyze particles function was used to count the number of pixels above the threshold in a region that was defined by an oval shape. This oval shape represented the concave region of the spermatid head where apical TBCs are located. The size of the oval shape remained constant for the measurements of all experiments. The total number of pixels above threshold was used as an index of the amount of actin network present in regions containing the TBC clusters.

Statistics

The 20 μM fluorescence experiment was performed once and the 40 μM experiment was done twice. A one-tailed, unpaired *t*-test with Welch correction was used to determine significant differences between experimental and control groups within each experiment. The 10 μM experiment could not be quantified because of differences in the variables of the imaging process.

Electron Microscopy

Drug-treated and control testes were perfused with a fixative containing 1.5% paraformaldehyde, 0.1 M sodium cacodylate (Electron Microscopy Sciences), and 1.5% glutaraldehyde (Electron Microscopy Sciences) adjusted to pH 7.3 rather than the fixative described above for fluorescence microscopy. After fixation for 30 min by perfusion, the testes were cut into small pieces and submerged in the same fixative for another 2–3 h. The tissue was washed three times for 10 min each with 0.1 M sodium cacodylate at pH 7.3 and then postfixed for 1 h on ice in 0.1 M sodium cacodylate and 1% osmium tetroxide (Electron Microscopy Sciences). The tissue was washed three times for 10 min each with double-distilled water (ddH_2O), stained for 1 h with uranyl acetate (Canemco-Marivac Inc.), washed another three times with ddH_2O, and then dehydrated using a series of ascending concentration series (30%, 50%, 70%, 95%, 100%) of ethanol solutions. The ethanol was replaced with propylene oxide (two washes, 30 min each, with 100% propylene oxide) and then the tissue was left overnight in a mixture of 1:1 propylene oxide and EMbed-812 (Electron Microscopy Sciences). The following day the tissue was embedded in 100% EMbed-812 and the samples polymerized at 60°C for 48 h. The blocks were sectioned and then the sections were stained with both uranyl acetate and lead citrate.

For obtaining images of normal tissue not treated with drug or control solutions, testes were excised as described above and then immediately perfused for 30 sec with PBS to clear the blood from the testes. The testes were fixed and prepared for electron microscopy as described above.

Stained sections were imaged using a Tecnai G2 Spirit electron microscope (FEI North America NanoPort) operated at 120 kV.

Qualitative observations of the drug experiments were made while scanning sections on the microscope and on the basis of a total of 377 digital images. Electron micrographs presented in the figures are representative images. Quantitative data for the diameters of TBCs were made on an additional 153 images taken specifically for that purpose.

Quantification of TBC Proximal Tubule Diameters

Two previously unsectioned blocks of embedded tissue were sectioned for each treatment and control testis for each experiment, and images collected for quantifying the diameters of the proximal tubular regions of TBCs. Images were taken of proximal tubules from different clusters of complexes in sections from each block (total of 12 blocks, 2 each for each of the control and experimental testes from the three animals; one animal for each dose). Each TBC was photographed at 68 000× on the microscope. The diameters of tubular regions were measured using ImageJ software version 1.48. A one-tailed, unpaired *t*-test with Welch correction was used to test for significant differences between the diameters of the tubular regions in experimental and control groups.

RESULTS

Seminiferous Epithelial Architecture Appears Normal in Cytochalasin D-Treated Tissue

Perfusion for 1 h with 10–40 μM cytochalasin D did not disrupt the overall structure of the seminiferous epithelium. At stage VII of spermatogenesis, late spermatids remained at the apex of the epithelium and were not sloughed or released. Cells deeper in the epithelium also did not detach from the epithelium. When stained with fluorescently tagged phalloidin, labeling of actin filaments at adhesion junctions (ectoplasmic specializations) associated with late spermatids appeared less intense in sections of drug-treated tissues than in controls, but was still detectable, as was labeling of filaments in ectoplasmic specializations at basal junctions between Sertoli cells.

Cytochalasin D Reduces the Area Occupied by Filamentous Actin Associated with Apical Clusters of TBCs

The amount of filamentous actin associated with clusters of TBCs in Sertoli cell cytoplasm adjacent to late spermatids appeared reduced in drug-treated epithelium relative to controls. In drug-treated clusters, the lengths of the actin cuffs appeared progressively shorter with increasing concentrations of cytochalasin D (Figs. 1, A′–D′, and 2, A, A′, B, and B′). When analyzed using thresholding techniques, there was a significant difference in the number of pixels above threshold between control and experimental groups for the 20 μM experiment ($P = 0.0019$) and each of the two 40 μM experiments ($P < 0.0001$; $P < 0.0003$) (Fig. 2C).

Cytochalasin D Treatment Disrupts Tubulobulbar Actin Cuffs

When analyzed at the ultrastructural level, the actin cuffs associated with tubular regions of the membrane core were less uniform in drug-treated tissues than in controls. In cross sections of TBCs in control tissues (Fig. 3A), the actin cuffs were most dense near the membrane core and gradually became less dense peripherally. In addition, the cuffs among complexes were all of uniform diameter and appearance. In drug-treated material, the actin cuffs appeared patchy with the filaments organized into distinct foci around the membrane core (Fig. 3B). These foci also occurred in regions dissociated from the membrane cores (Fig. 3, C–E).

Actin Disruption Results in Swollen Tubular Regions, Ectopic Bulbs, Malformations, and Shorter Complexes

In tissue treated with cytochalasin D, tubular regions of the complexes appeared swollen when visualized both in cross sections (Fig. 3B) and in longitudinal sections (Fig 4, A–D) of TBCs. In control tissues, the proximal tubular regions appeared uniform in diameter and were surrounded by a continuous actin cuff along their lengths (Fig. 4A). In drug-treated material, the diameters of the tubules were enlarged (compare Fig. 4A with Fig. 4C; notice that Fig. 4A is at a higher magnification than Fig. 4C) and the actin cuffs were less obvious and patchy. When proximal tubule diameters were measured in each of the 10, 20, and 40 μM experiments, there was a significant difference in diameters between control and drug-treated testes (Fig. 5).

In addition to swollen tubular regions, ectopic bulbs were present in cytochalasin D-treated material. In control tissues, the bulbs of TBCs were positioned in their normal location at the ends on elongate tubules close to the coated pits (Fig. 6A). The bulbs were easily identified by their large diameters relative to tubular regions and their close association with cisternae of endoplasmic reticulum. In drug-treated testes, ectopic bulbs were often observed near the bases of TBCs, where they emerged from areas of attachment to spermatid heads (Fig. 6, B–D).

Malformed TBCs also were observed in actin-disrupted material. Control complexes looked normal with elongate proximal tubules, bulbs, and a single coated pit at their end (Fig. 7A). Among the misshaped complexes observed were those with multiple coated pits at their ends (Fig. 7B) and those with one or more branches along their lengths (Fig. 7, C and D).

In addition to being swollen and malformed, TBCs in drug-treated tissues appeared shorter overall than in controls (Figs. 6 and 7D).

Absence of Tubular Regions and Enlarged Bulbs

Occasionally, massively enlarged bulbs were observed in cytochalasin D-treated material that occupied virtually the entire length of the complexes (Fig. 8, A and B); in other words, elongate proximal tubules with actin cuffs were absent. In many of these cases, short distal tubular regions that

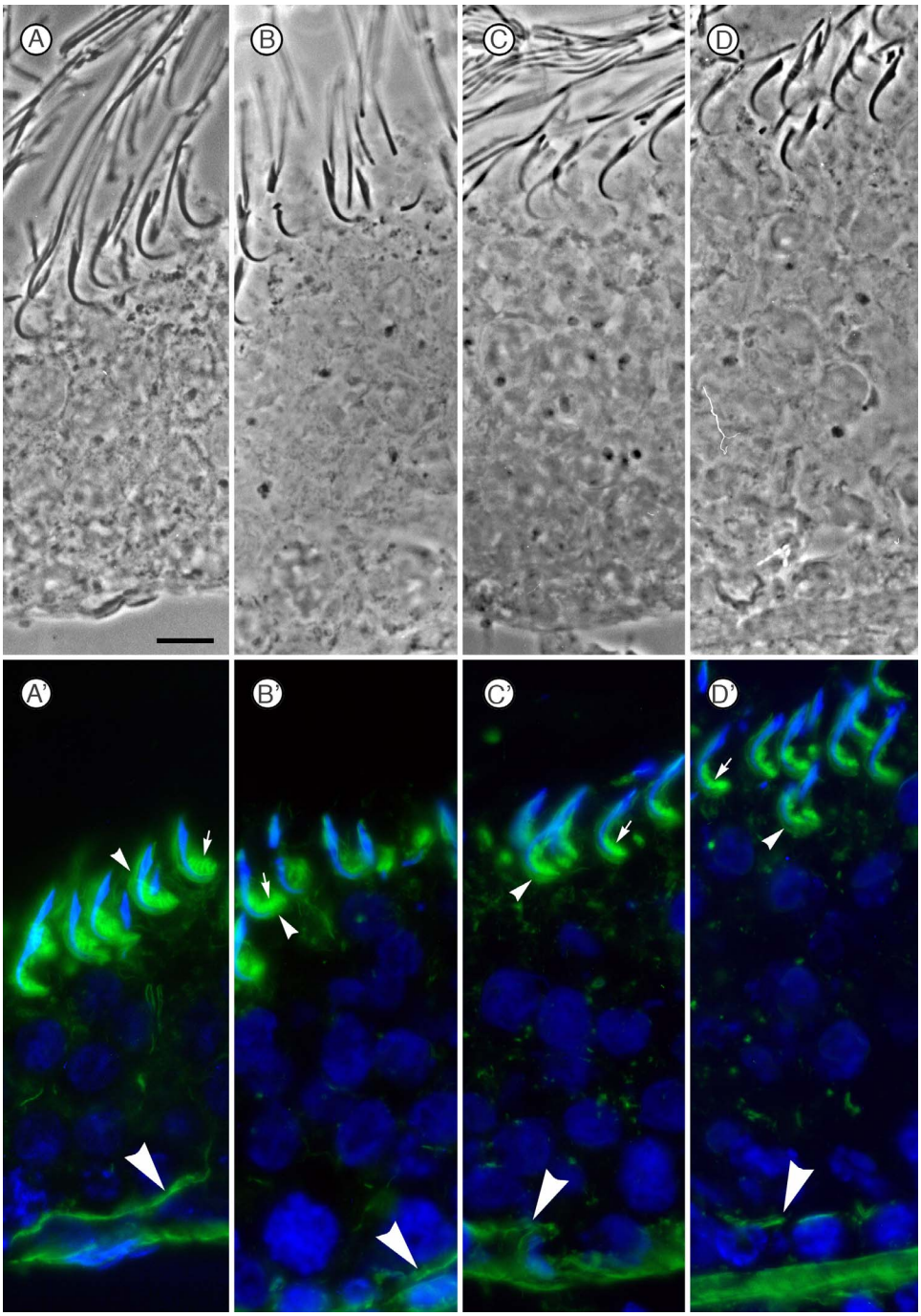

FIG. 1. Paired fluorescence and phase images of stage VII seminiferous epithelium from rat testes perfused for 1 h with control buffer (**A**, **A′**) or with buffer containing 10 (**B**, **B′**), 20 (**C**, **C′**) or 40 μM (**D**, **D′**) cytochalasin D. In each case the sections have been labeled for filamentous actin with fluorescent phalloidin (green) and for DNA with DAPI (blue). Actin staining in basal (large arrowheads) and apical (small arrowheads) ectoplasmic specializations is present, as is staining of the actin networks associated with TBCs (arrows) adjacent to the concave surface of late spermatids situated at the apex of the epithelium. Notice that the epithelium appears intact even after treatment with the highest dose of cytochalasin D and there is no cell detachment or sloughing. Also notice that the actin labeling in regions associated with TBCs does not extend as far away from the spermatid head in cytochalasin D-treated epithelia as in controls. Bar = 10 μm.

normally occur between the bulbs and coated pits, and that also have actin cuffs, were absent as well (Fig. 8, A and B).

Large Bulbs and Short Tubular Regions Occur in Untreated Early Stage VII Tubules

In tubules from untreated testes that were excised from animals and immediately perfusion fixed, large elongate and folded bulbs with short tubular regions were observed (Fig. 9, A and B). These TBCs somewhat resembled those from late stage VII complexes exposed to cytochalasin D (Fig. 8, A and B).

DISCUSSION

In this study we show that disrupting the actin networks of TBCs results in increased diameters of tubular regions, the

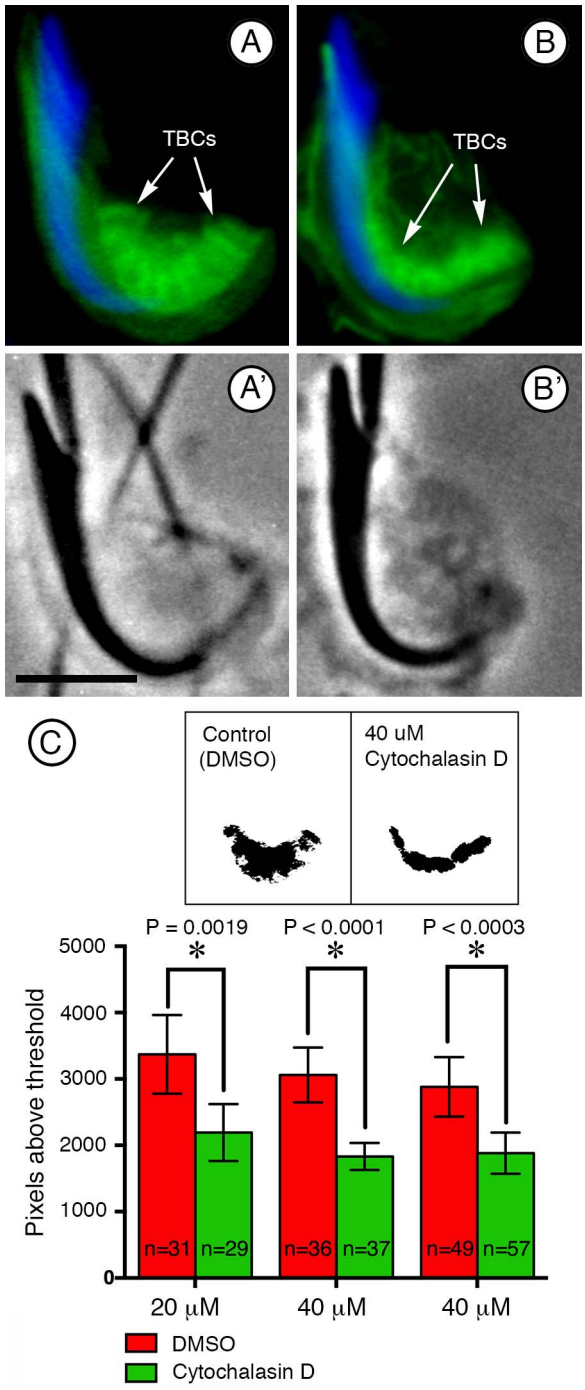

FIG. 2. Less actin is associated with apical TBCs in cytochalasin D-treated epithelia compared to controls. Shown in **A**, **A′**, **B**, and **B′** are paired fluorescence and phase images of apical processes of Sertoli cells surrounding late spermatid heads from control and cytochalasin D-treated (40 μM) testes respectively. Bar = 5 μm. The samples have been labeled with fluorescent phalloidin for filamentous actin (green) and DAPI (blue) for DNA. Actin associated with clusters of TBCs is not as extensive in drug-treated material as in controls, and the actin cuff of each complex is shorter. The graph in **C** shows the numbers of pixels above threshold in control and drug-treated (one 20 μM and two 40 μM cytochalasin D experiments) tubulobulbar clusters associated with late spermatid heads. The inset in **C** is an example of the pixels above threshold in tubulobulbar regions of a control and a cytochalasin-treated apical Sertoli cell process. Data are expressed as mean ±95% confidence intervals. Asterisks indicate significant differences ($P < 0.05$).

formation of ectopic bulbs, and the presence of branched complexes. The results are consistent with the conclusion that intact actin networks are necessary for maintaining the structural integrity of TBCs. Based on our observations of TBCs in cytochalasin D-treated testes, together with observations of the structures in untreated epithelium, we propose a new model for how mature TBCs may be internalized by Sertoli cells.

TBCs were originally identified and their overall structure defined in a series of classic studies by Russell and coworkers [6, 8, 9]. The structures begin as coated pits that project into Sertoli cells at sites of intercellular attachment in the mammalian seminiferous epithelium. The plasma membranes of the two cells remain attached as the pits mature, and the necks of the structures do not undergo scission to form vesicles. Rather, the necks continue to elongate, forming long double-membrane tubes, each surrounded by a cuff of actin filaments that in turn is surrounded by a cytoskeletal shell consisting of plectin (PLEC) and spectrin (SPT-) [24]. These complexes extend up to 2–3 μm into Sertoli cells in rats [6], and up to 6–8 μm in opossums [9]. As TBCs mature, swellings (bulbs) develop near the ends of the complexes. The bulbs eventually dissociate from the complexes and are degraded by Sertoli cells [8] as part of the mechanism of junction remodeling that precedes sperm release at the apex of the epithelium and translocation of spermatocytes through basal junction complexes at the base of the epithelium [4]. The precise function of the actin filament cuffs surrounding tubular regions of TBCs is not known, nor is it known how the actin networks are related to formation and scission of the bulbs.

In clathrin-associated endocytosis generally in cells, actin filament networks have been implicated in invaginating the coated pits, constricting the necks of forming vesicles, scission of the vesicles from the plasma membrane, and moving the internalized vesicles deeper into the cytoplasm [14, 25]. Actin has been found to recruit and facilitate the assembly of dynamin (DNM-) during formation of the neck and to promote dynamin-mediated vesicle scission [26]. In dynamin knockout cells, coated pits with very long, narrow necks are formed and scission does not occur [27]. In these same cells treated with latrunculin B to prevent actin polymerization by sequestering G-actin, elongate necks do not form and coated pits remain attached to the plasma membrane by wide necks. Together these results indicate that in clathrin-mediated endocytosis, an intact actin cytoskeleton participates in the formation of constricted necks and in scission of vesicles from the plasma membrane. When dynamin-mediated scission does not occur, continued actin polymerization results in abnormally long necks.

In the testis, Russell and coworkers [19] report the complete absence of normal TBCs at apical sites in rat seminiferous epithelium 3 h post-intratesticular injection of 50 μl of 500 μM cytochalasin D. What occurs instead are numerous double-membrane coated pits directly associated with attachment sites between Sertoli cells and spermatids. In other words, tubular and bulbar regions are absent. Although these results are somewhat difficult to interpret because 1) the time it takes for any single TBC to develop is not known and 2) the period during which TBCs are present at apical sites in the epithelium spans 3–4 days, the results are generally consistent with the conclusion that actin filaments are necessary for development and elongation of the tubular regions. Our results, using ex vivo testicular perfusion methods to control drug dosage, extend these earlier results and provide insight into the formation and eventual scission of the bulbs.

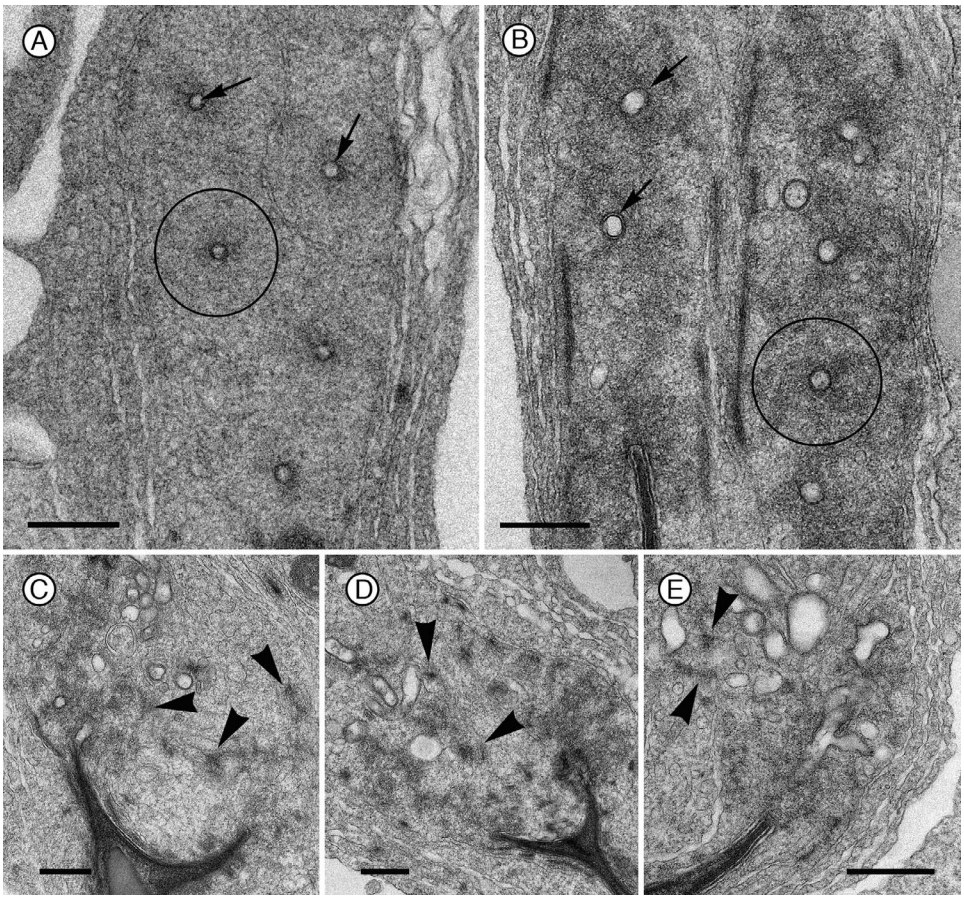

FIG. 3. Electron micrographs of actin networks associated with TBCs in control and cytochalasin D-treated testes. Compared to controls (**A**), the actin filaments associated with TBCs appear patchy (**B**, 40 μM cytochalasin D), occur in dense foci (**C** and **D**, 40 μM cytochalasin D), and appear less organized (**E**, 40 μM cytochalasin D). Arrows in **A** and **B** indicate the membrane cores of TBCs in cross section. The black circles outline the approximate boundaries of the actin cuffs surrounding the membrane cores. The arrowheads in **C**–**E** indicate actin foci in Sertoli cell regions containing TBCs. Bars = 500 nm.

In the experiments reported here, perfusion with cytochalasin D did not result in disruption of overall epithelial architecture. When fluorescent phalloidin was used to label actin filaments, the characteristic pattern of staining at apical and basal intercellular junctions in the epithelium was still present, although somewhat weaker than in controls. In addition, no detachment of cells from the epithelium was detected at any of the dosages.

Although there were no dramatic changes in epithelial architecture with cytochalasin D exposure, we did observe major effects of the drug treatment on TBCs. The amount of actin network associated with apical TBC clusters was significantly different in drug-treated testes compared to controls, and individual complexes appeared shorter. When evaluated at the ultrastructural level, the diameters of tubular regions appeared larger. When quantified, there was a significant difference in proximal tubule diameters between control and drug-treated testes at each of the doses of drug tested. In addition, ectopic bulbs were present, and the complexes often appeared branched and malformed. Distal tubular regions appeared absent in many cases and the coated pits were directly associated with the bulbs or swollen regions of the complexes. We conclude that actin cuffs are necessary for maintaining the normal structure of tubular regions.

Potentially the most significant result of our study is that when the actin filament networks of TBCs are disrupted, the tubular regions swell and form bulbs.

The currently accepted model for internalization of a TBC is one in which there are multiple scission sites along the structure that result in not only internalization or budding of the bulb but also internalization of the coated pit from the end of the complex and numerous vesicles resulting from fragmentation of the proximal tubule [20] (Fig. 10A) In part, this model arose from the early ultrastructural observation that vesiculation of the inner spermatid membrane tube occurred within the proximal tubule of apical TBCs [6, 8]. If this model for internalization of TBCs is true, one might predict an abundance of small double-membrane vesicles in Sertoli cell regions where TBCs occur, and that some of these vesicles would appear to have dense cores resulting from the submembrane densities associated with the spermatid plasma membranes in the coated pits. Neither of these features is obvious in tubulobulbar-containing regions of the Sertoli cell.

Our results together with the earlier observations of Russell and coworkers [19] suggest the following alternative model for formation of the bulb and internalization of a TBC by the Sertoli cell (Fig. 10B). Polymerization of actin filaments drives the elongation of the TBC and projects it deep into the Sertoli cell. In addition to growth of the complex, the actin cuff also participates in maintaining the narrow diameter of the double-membrane tubule. Focal loss of the actin cuff near the end of each complex initiates the formation of a bulb. We predict that other components known to be present at TBCs, such as the BAR domain proteins [28] and dynamin [20, 28], also detach from this region of the tubule as the bulb forms. As the actin

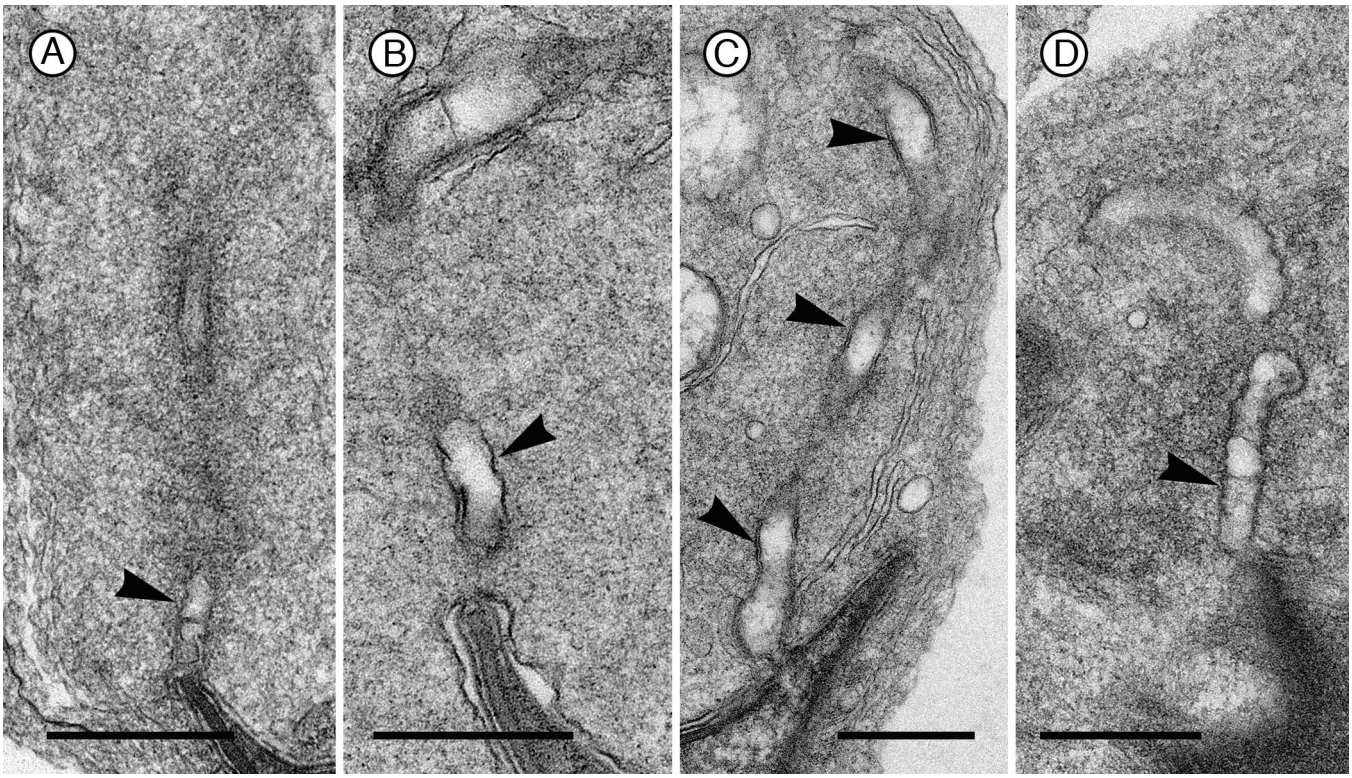

FIG. 4. Relative to controls (**A**), tubular regions of apical TBCs (arrowheads) are swollen in cytochalasin D-treated epithelia (**B**–**D**, 10, 20, and 40 μM cytochalasin D, respectively). Bars = 500 nm.

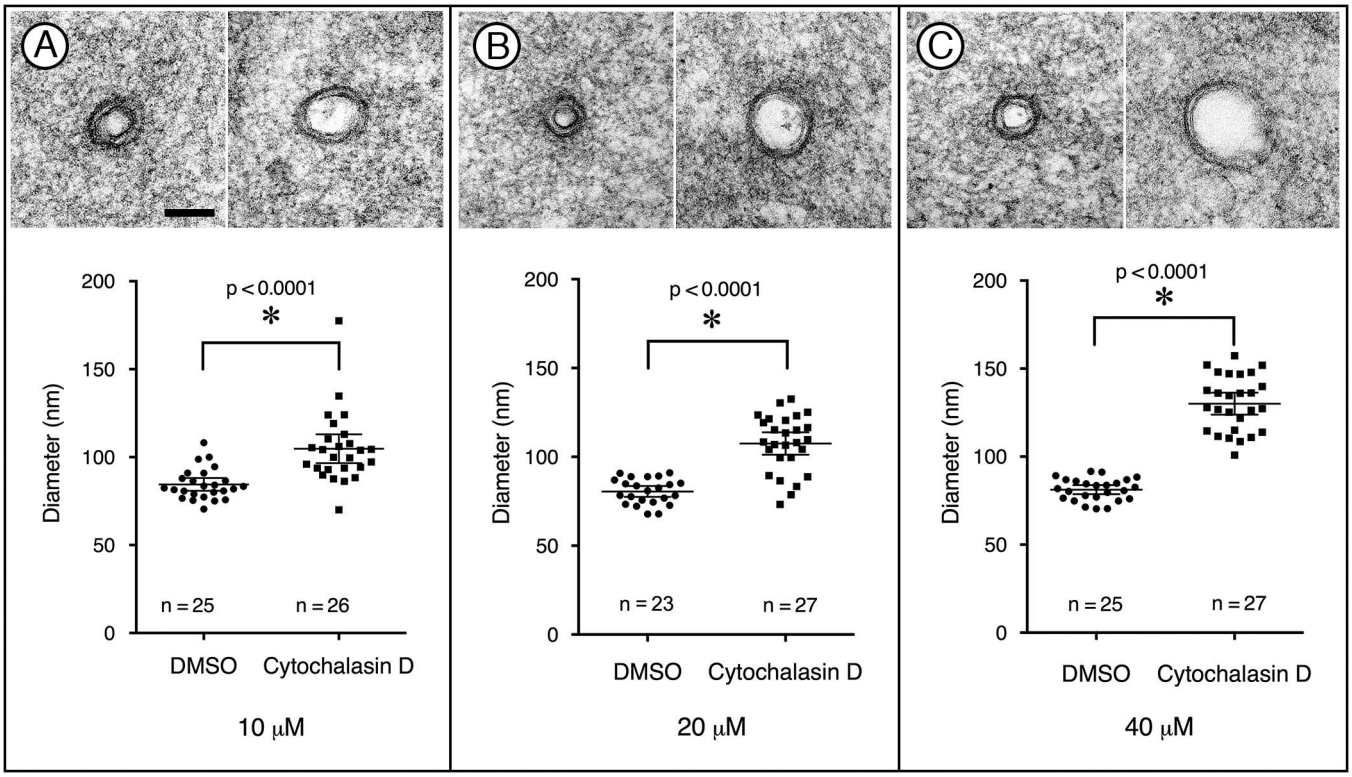

FIG. 5. Cytochalasin D treatment results in an increased diameter of the proximal tubules of TBCs. Shown here are results from each of the single experiments done with 10 (**A**), 20 (**B**), and 40 (**C**) μM cytochalasin D. Shown in the graphs are all the individual data points, the means, and the 95% confidence intervals. In each experiment there is a significant difference between control (DMSO) and cytochalasin D-treated testes. The electron microscopic images above each of the graphs are representative sections through the proximal tubular region of TBCs in control (left panels) and drug-treated (right panels) testes. Bar = 100 nm.

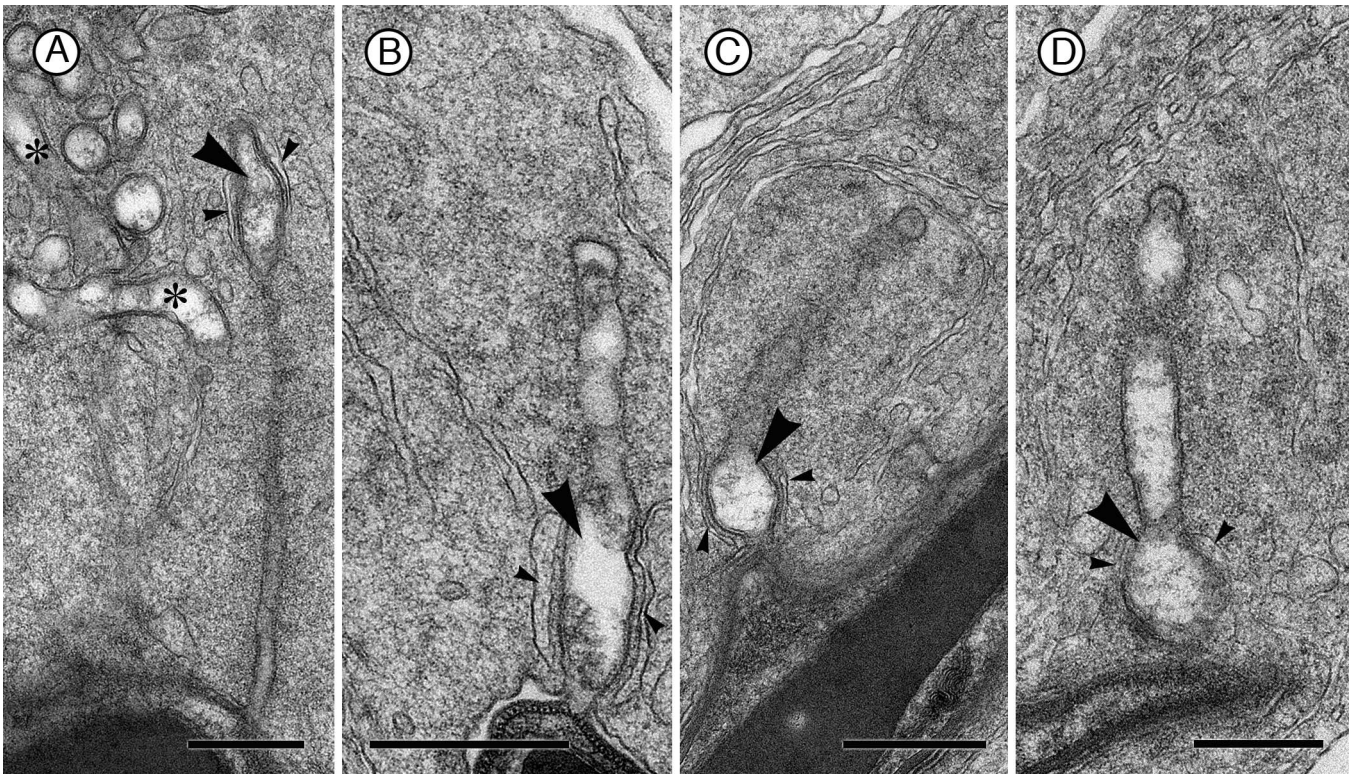

FIG. 6. Ectopic bulbar regions occur in TBCs from cytochalasin D-treated epithelia. A normal TBC from control epithelium is shown in **A**. Here, a bulb (large arrowhead) appears near the distal end of the complex and is characterized by closely related cisternae of endoplasmic reticulum (small arrowheads). Also notice that some of the bulbs, indicated by the asterisks, are elongate (cigar-shaped) and somewhat folded. In drug-treated samples, ectopic bulbs (large arrowheads) occur often near proximal regions of the complexes (**B**–**D**, 10, 20, and 20 μM cytochalasin D, respectively). Cisternae of endoplasmic reticulum associated with the bulbs are indicated by the small arrowheads in all panels. Bars = 500 nm.

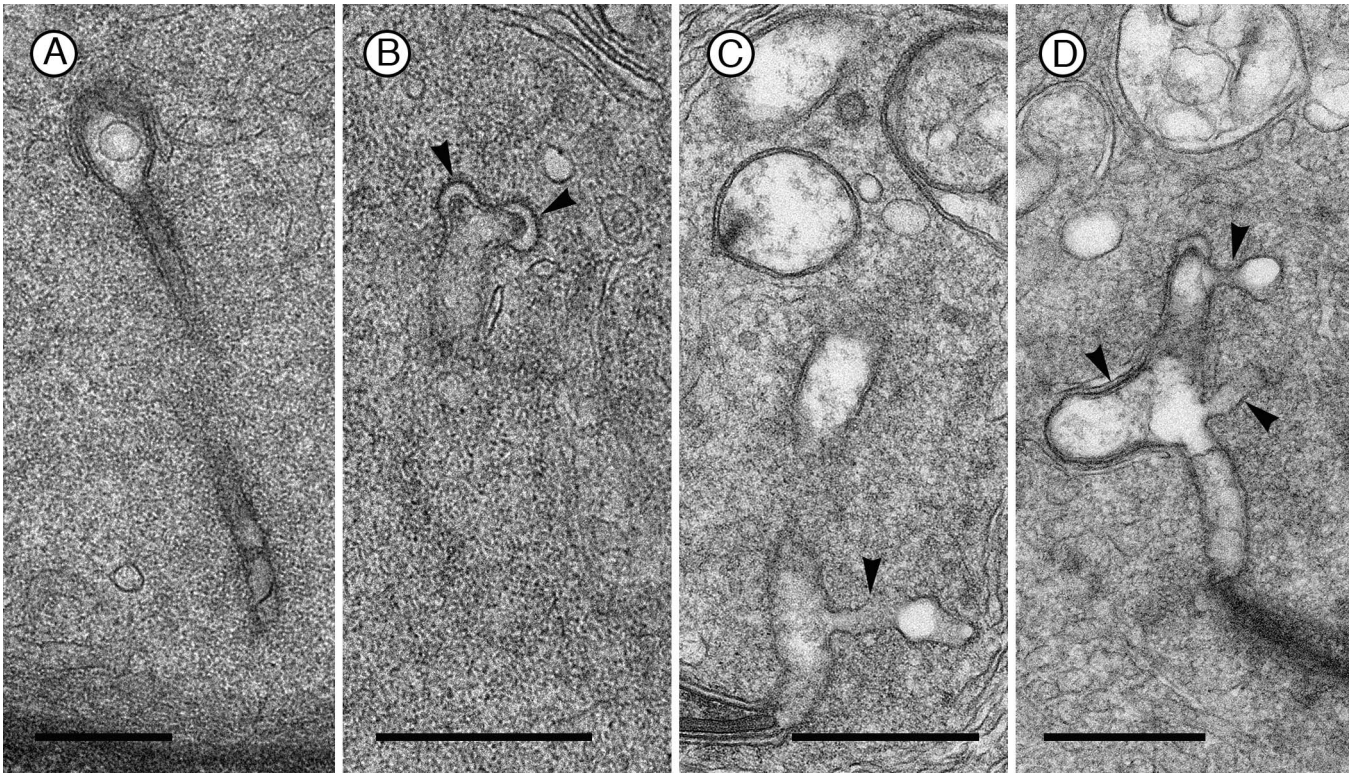

FIG. 7. Cytochalasin D treatment results in TBCs with abnormal morphology. Shown in **A** is a normal-appearing TBC with a long proximal tubular region and a distal bulb. Shown in **B** (10 μM cytochalasin D) is the distal end of a complex with two coated pits (arrowheads) rather than the normal one. In **C** (20 μM cytochalasin D) and **D** (40 μM cytochalasin D) are swollen and branched (arrowheads) complexes. Bars = 500 nm.

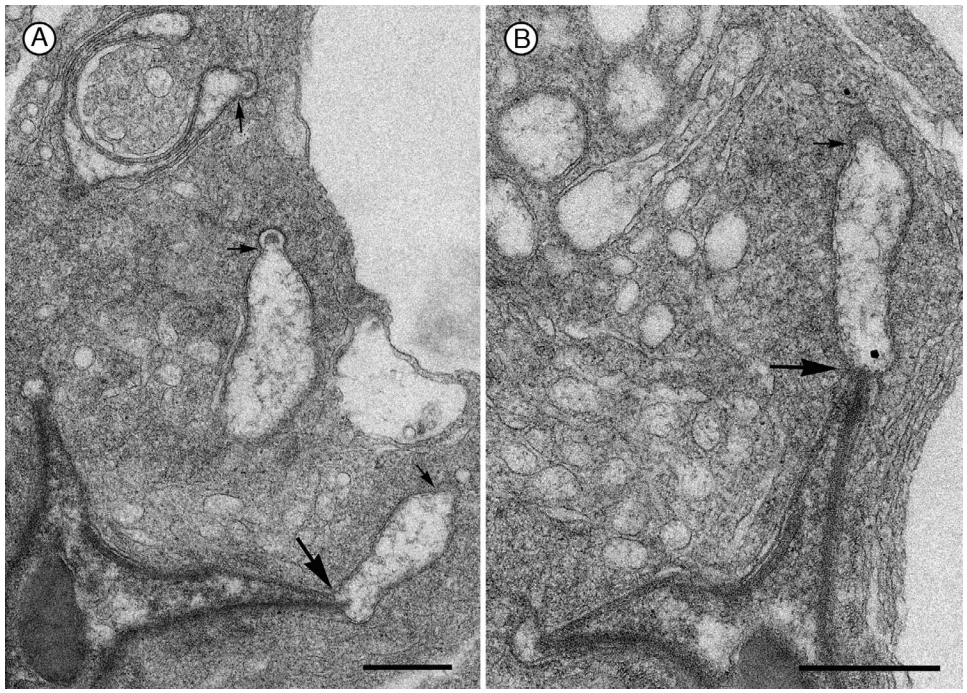

FIG. 8. **A** and **B**) Shown here are dramatically swollen TBCs from epithelia treated with 40 μM cytochalasin D. The large arrows in each panel indicate the absence of proximal tubular regions and the small arrows indicate the absence of distal tubular regions. Bars = 500 nm.

cuff is lost, cisternae of endoplasmic reticulum associate directly with the Sertoli cell plasma membrane of the forming bulb. Continued loss of the actin cuff and related proteins, both proximal and distal to the initiation site, expands the bulb. This expansion or elongation of the bulb eventually incorporates or resolves the coated pit into its structure distally, and reduces the length of the proximal tubule until only a small ''neck'' remains near the site where the complex originates from the intercellular junction. The possibility that the coated pit is resolved into the bulb may not be entirely without precedent because not all clathrin-coated structures that form generally in cells proceed to separation from the plasma membrane [13]. Scission, possibly regulated by dynamin remaining at the site, occurs at the small neck and results in the bulb being

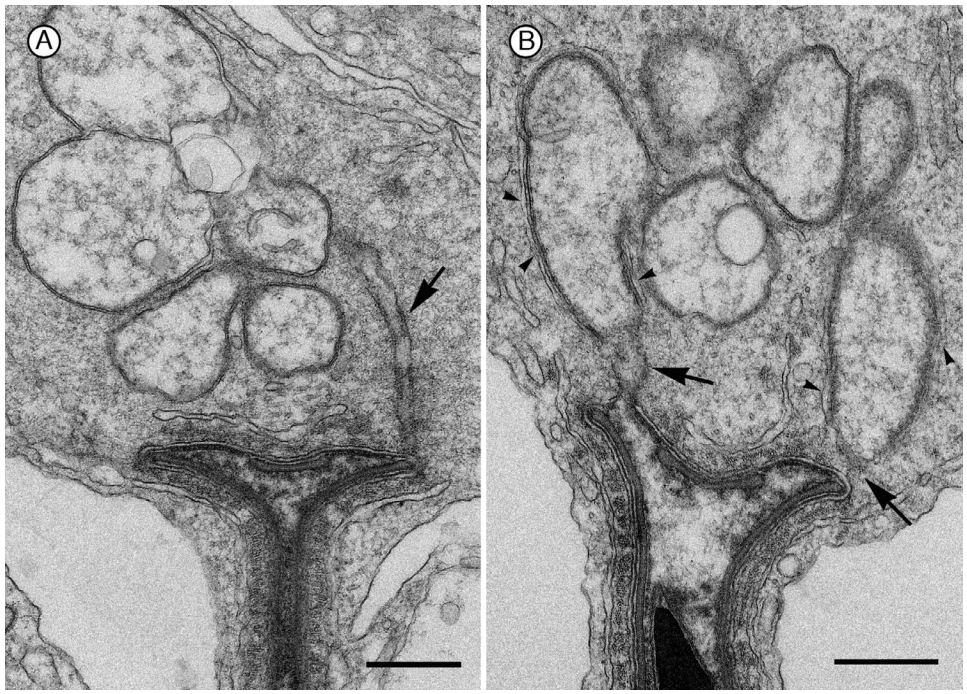

FIG. 9. Tubulobulbar regions from untreated seminiferous epithelia at early stage VII of the seminiferous epithelium. Notice that the bulbs are large in **A** and have lost the association with cisternae of endoplasmic reticulum. A proximal tubular region is present (indicated by the arrow). In **B** proximal tubular regions are short or absent (arrows). Cisternae of endoplasmic reticulum associated with the bulbs are indicated by the arrowheads. Bars = 500 nm.

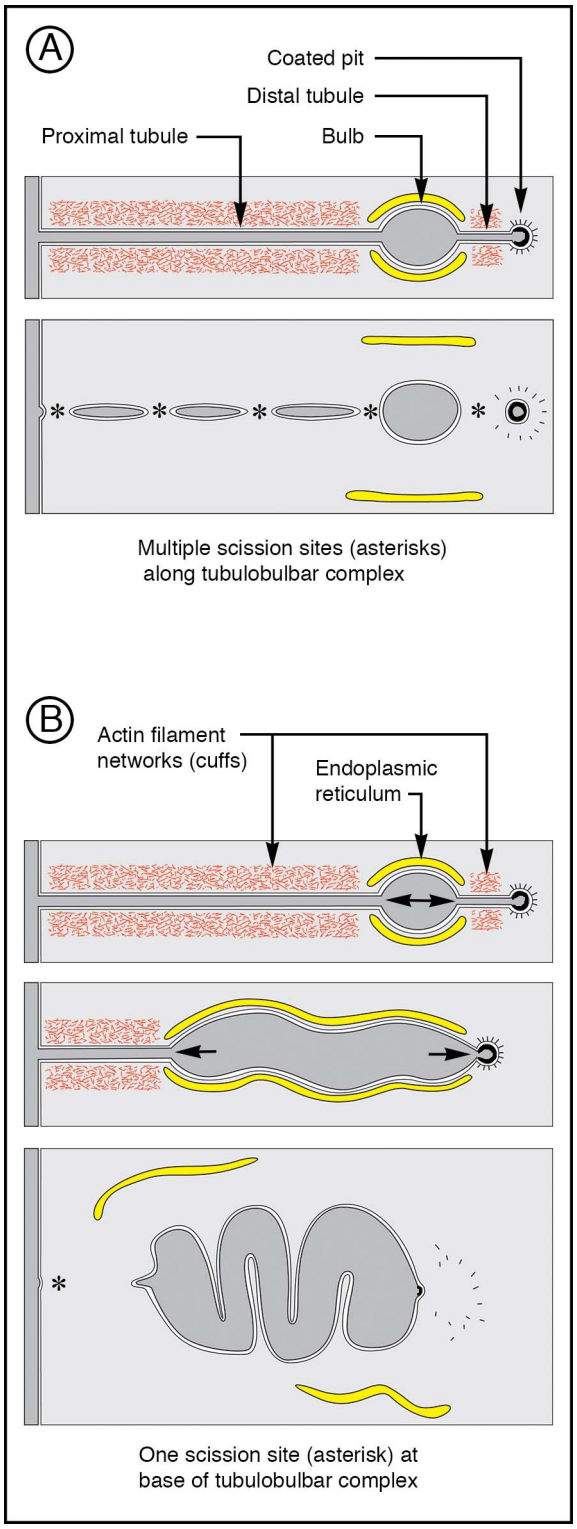

FIG. 10. Models of tubulobulbar vesiculation. In model **A**, the bulb buds from the complex and the remaining tubular regions and coated pit undergo scission to form multiple vesicles. In model **B**, the actin networks of the proximal and distal tubules progressively disassemble and the bulb region enlarges to incorporate the coated pit and most of the proximal tubule. Eventually, the remaining short segment of the proximal tubule region near the base of the complex, or neck of the bulb, undergoes scission and the bulb is internalized and trafficked to endocytic compartments of the Sertoli cell.

internalized into the Sertoli cell. This model is attractive because it involves only one scission site, and is consistent with the appearance of enlarged bulbs in early stage VII (see Fig. 9B) of spermatogenesis, and with the elongate and folded cigar-shaped bulbs often seen later in stage VII (see Fig. 6A). Live cell imaging of TBC formation and internalization using epithelial fragments (for apical complexes), or perhaps primary Sertoli cell culture systems (for basal complexes), could eventually be used to discriminate between the two models.

REFERENCES

1. Russell L. Movement of spermatocytes from the basal to the adluminal compartment of the rat testis. Am J Anat 1977; 148:313–328.
2. Dym M, Fawcett DW. The blood-testis barrier in the rat and the physiological compartmentation of the seminiferous epithelium. Biol Reprod 1970; 3:308–326.
3. Vogl AW, Young JS, Du M. New insights into roles of tubulobulbar complexes in sperm release and turnover of blood-testis barrier. Int Rev Cell Mol Biol 2013; 303:319–355.
4. Vogl AW, Du M, Wang XY, Young JS. Novel clathrin/actin-based endocytic machinery associated with junction turnover in the seminiferous epithelium. Semin Cell Dev Biol 2014; 30:55–64.
5. Russell LD, Goh JC, Rashed RM, Vogl AW. The consequences of actin disruption at Sertoli ectoplasmic specialization sites facing spermatids after in vivo exposure of rat testis to cytochalasin D. Biol Reprod 1988; 39:105–118.
6. Russell L, Clermont Y. Anchoring device between Sertoli cells and late spermatids in rat seminiferous tubules. Anat Rec 1976; 185:259–278.
7. Russell LD. Observations on the inter-relationships of Sertoli cells at the level of the blood- testis barrier: evidence for formation and resorption of Sertoli-Sertoli tubulobulbar complexes during the spermatogenic cycle of the rat. Am J Anat 1979; 155:259–279.
8. Russell LD. Further observations on tubulobulbar complexes formed by late spermatids and Sertoli cells in the rat testis. Anat Rec 1979; 194: 213–232.
9. Russell LD, Malone JP. A study of Sertoli-spermatid tubulobulbar complexes in selected mammals. Tissue Cell 1980; 12:263–285.
10. Young JS, Guttman JA, Vaid KS, Shahinian H, Vogl AW. Cortactin (CTTN), N-WASP (WASL), and clathrin (CLTC) are present at podosome-like tubulobulbar complexes in the rat testis. Biol Reprod 2009; 80:153–161.
11. Ochoa GC, Slepnev VI, Neff L, Ringstad N, Takei K, Daniell L, Kim W, Cao H, McNiven M, Baron R, De Camilli P. A functional link between dynamin and the actin cytoskeleton at podosomes. J Cell Biol 2000; 150: 377–389.
12. Wu M, Huang B, Graham M, Raimondi A, Heuser JE, Zhuang X, De Camilli P. Coupling between clathrin-dependent endocytic budding and F-BAR-dependent tubulation in a cell-free system. Nat Cell Biol 2010; 12: 902–908.
13. Taylor MJ, Perrais D, Merrifield CJ. A high precision survey of the molecular dynamics of mammalian clathrin-mediated endocytosis. PLoS Biol 2011; 9:e1000604.
14. Kaksonen M, Toret CP, Drubin DG. Harnessing actin dynamics for clathrin-mediated endocytosis. Nat Rev Mol Cell Biol 2006; 7:404–414.
15. Kaksonen M, Toret CP, Drubin DG. A modular design for the clathrin- and actin-mediated endocytosis machinery. Cell 2005; 123:305–320.
16. Schafer DA, Weed SA, Binns D, Karginov AV, Parsons JT, Cooper JA. Dynamin2 and cortactin regulate actin assembly and filament organization. Curr Biol 2002; 12:1852–1857.
17. Merrifield CJ, Perrais D, Zenisek D. Coupling between clathrin-coated-pit invagination, cortactin recruitment, and membrane scission observed in live cells. Cell 2005; 121:593–606.
18. Young JS, de Asis M, Guttman JA, Vogl AW. Cortactin depletion results in short tubulobulbar complexes and spermiation failure in rat testis. Biol Open 2012; 1:1069–1077.
19. Russell LD, Saxena NK, Turner TT. Cytoskeletal involvement in spermiation and sperm transport. Tissue Cell 1989; 21:361–379.
20. Vaid KS, Guttman JA, Babyak N, Deng W, McNiven MA, Mochizuki N, Finlay BB, Vogl AW. The role of dynamin 3 in the testis. J Cell Physiol 2007; 210:644–654.
21. Hoffer AP, Carlton BD, Brunengraber H. Ultrastructure and intercellular vacuolization of isolated perfused and control rat testes. J Androl 1983; 4: 361–370.
22. Russell LD, Saxena NK, Weber JE. Intratesticular injection as a method to

assess the potential toxicity of various agents and to study mechanisms of normal spermatogenesis. Gamete Res 1987; 17:43–56.
23. Abramoff MD, Magalhaes PJ, Ram SJ. Image processing with ImageJ. Biophotonics Int 2004; 11:36–42.
24. de Asis MA, Pires M, Lyon K. A network of spectrin and plectin surrounds the actin cuffs of apical tubulobulbar complexes in the rat. Spermatogenesis 2013; 3:e25733.
25. Collins A, Warrington A, Taylor KA, Svitkina T. Structural organization of the actin cytoskeleton at sites of clathrin-mediated endocytosis. Curr Biol 2011; 21:1167–1175.
26. Grassart A, Cheng AT, Hong SH, Zhang F, Zenzer N, Feng Y, Briner DM, Davis GD, Malkov D, Drubin DG. Actin and dynamin2 dynamics and interplay during clathrin-mediated endocytosis. J Cell Biol 2014; 205: 721–735.
27. Ferguson SM, Raimondi A, Paradise S, Shen H, Mesaki K, Ferguson A, Destaing O, Ko G, Takasaki J, Cremona O, O'Toole E, De Camilli P. Coordinated actions of actin and BAR proteins upstream of dynamin at endocytic clathrin-coated pits. Dev Cell 2009; 17:811–822.
28. Kusumi N, Watanabe M, Yamada H, Li SA, Kashiwakura Y, Matsukawa T, Nagai A, Nasu Y, Kumon H, Takei K. Implication of amphiphysin 1 and dynamin 2 in tubulobulbar complex formation and spermatid release. Cell Struct Funct 2007; 32:101–113.